Kim, S.R., Chung, S.G., and Fellenius, B.H., 2011. Distribution of residual load and true shaft resistance for a driven instrumented test pile. Canadian Geotechnical Journal, (48)4 583-598.

Distribution of Residual Load and True Shaft Resistance for a Driven Instrumented Test Pile

Sung-Ryul Kim[1], Sung-Gyo Chung[1], and Bengt H. Fellenius[2],

[1] Dong-A University, Dept of Civil Engineering, 840 Hadan-dong, Saha-gu, Busan, 604-714 Korea
[1] Consulting Engineer, 2475 Rothesay Avenue, Sidney, BC, V8L 2B9

ABSTRACT To provide needed insight in the foundation conditions for a series of apartment buildings to be constructed in a shore area reclaimed from the Nakdong River estuary delta area west of Busan, South Korea, full-scale field tests were performed on two strain-gage instrumented, 600-mm, post-driving grouted, concrete cylinder piles. Both test piles were driven through the compressible layers and a short distance into underlying dense sand at depths of 56 m (Shinho site) and 35 m (Myeonji site). In order to allow unambiguous separation of shaft and toe resistances, one test pile was provided with an bidirectional-cell so that after an initial test, a subsequent head-down test only affected the pile shaft resistance. The purpose of the tests was to evaluate the drivability of the piles, to determine the magnitude of the drag load that would be caused by the consolidating soils, and to estimate the potential settlement (downdrag) of the piled foundations. Early in the study, it became apparent that the internal process of heating and cooling of the grout during the hydration process and swelling from absorption of water greatly affected the strain records, and the assessment of residual load in the test piles during the wait time before the static loading test. The paper reports the measurements and analyses and indicates the method for determining the residual load, the strain-dependent modulus of the test piles, and the actual load distribution in the test piles. The results are correlated to CPTU sounding data and effective stress analysis.

1. INTRODUCTION

The Nakdong River estuary delta area covers a large area west of the city of Busan, South Korea, and is composed of very thick deposits of compressible and, originally, normally consolidated clays with occasional interbedded sand layers. Two areas, called Shinho and Myeongji, were reclaimed starting in the early 1990s by placing fill to raise the land above flood levels. During the more than ten years following, these areas have been lying vacant due to high construction costs of the deep foundations required for all but light structures. Recently, however, because of space becoming increasingly limited in the city, tall apartment buildings are being designed and built in the area to house approximately 80,000 people.

The design has to take into account the ongoing consolidation settlement at the site, and that all major buildings require piled foundations because of the low bearing capacity of the deltaic soils. The commonly employed deep foundation system in Korea consists of steel pipe piles driven to significant toe bearing in dense soils or on bedrock. Where these piles become very long, such as the 70 m to 80 m lengths anticipated for the Nakdong River estuary delta, the foundations become very costly. For the subject development, an alternative pile type is considered: a cylindrical concrete pile, called PHC (Pre-tensioned spun High strength Concrete) piles. The in-place cost of a PHC pile is between a quarter to a third of the cost of a similar length steel pile. However, the PHC pile is considered less suited for the hard driving required to reach the termination depths usually selected for the steel piles. For the PHC pile to become a viable alternative, it is desirable to terminate the piles at a shallower depth, relying on shaft resistance and moderate toe resistance in intermediate sand layers at depths of about 30 m to 50 m. Before finalizing the design of the foundations, a full-scale investigation was carried out, as reported in this paper, to verify that the PHC pile can withstand the driving to the required capacity, has sufficient axial strength to accept the anticipated drag load, and is not subject to excessive downdrag.

A comprehensive full-scale testing programme involving the PHC pile was executed that included pile drivability with dynamic testing and static loading tests on two strain-gage instrumented test piles at two close-by sites, Myeongji and Shinho. The strain-gages were monitored during a five to seven months setup period, respectively and during the loading test. Because the expected capacity of the first test pile (at Myeongji) showed to be too large to be evaluated by a conventional head-down static loading test, the testing of the second pile (at Shinho) combined an initial bidirectional-cell test (Osterberg 1998) with the cell placed at the pile toe and a subsequent head-down loading test with the toe cell open to eliminate the toe resistance.

2. SITE CONDITIONS

The tests were carried out at the Myeongji and Shinho sites, located about 2 Km apart in the western part of the Nakdong River estuary close to the shore. Detailed descriptions of the soil deposit are given by Chung et al. (2002, 2005, 2007). Figure 1 shows the results of a CPTU sounding from the test site about 30 m away from the Shinho test pile. The soil profile consists of a 5 m to 8 m thick clayey sandy fill (density 1,900 kg/m^3) placed over an about 10 m thick layer of loose silty sand with interbedded layers of fine-grained soil (density 2,000 kg/m^3) followed by a 20 m to 35 m thick compressible layer of soft silty clay (density 1,750 kg/m^3), undergoing consolidation. Typically, the compression ratio, CR, for the soft clay ranges from 0.35 to 0.20— CR is equal to $C_c/(1+e_0)$ —the

Received by the Journal on June 1, 2009; accepted Sep. 1, 2010.

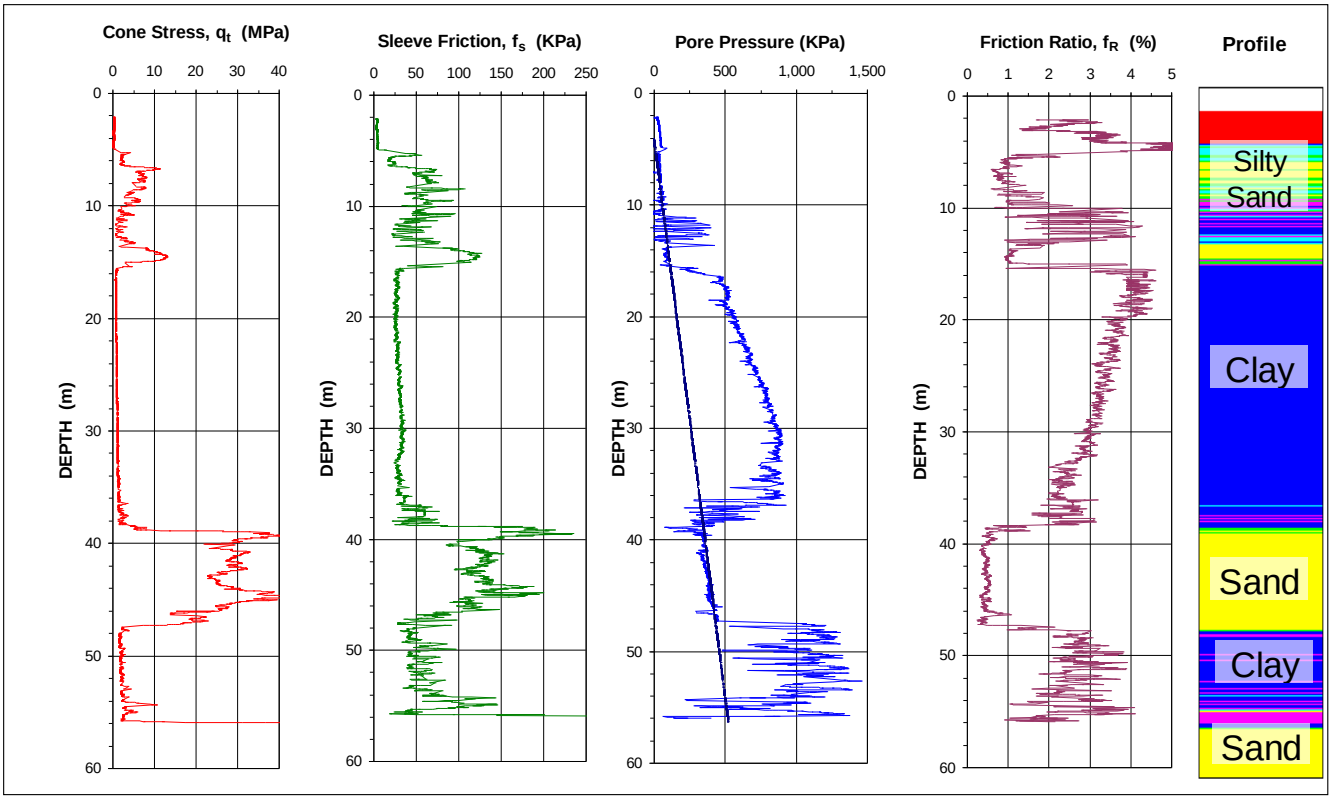

Fig. 1 CPTU at Shinho. Cone resistance, q_t, Sleeve Friction, f_s, Pore Pressures, U2 and u_0, and Friction Ratio f_R

CR range corresponds Janbu modulus numbers, m, ranging from 7 to 12 (m = 2.3/CR). Below the clay, at depths between about 38 m through 48 m, the soil consists of dense silty sand (density 2,050 kg/m^3), containing seams of silty clay as well as sand and sandy gravel. Over a large portion of the Shinho site, a zone of soft to firm silty clay is interbedded with the silty sand (density 2,050 kg/m^3). Its compression ratio, CR, is typically 0.2 (modulus number, m, of 12). Below the silty sand, starting at depths of about 55 m to 75 m, the soil consists of very dense sand and gravel. The cone penetration test at the Shinho site was terminated on reaching 200 mm into the surface of the latter layer at cone stress of 48 MPa at a total depth of 56.3 m. The CPTU inclination measurements show that the actual depth of the cone at termination was 0.25 m smaller than recorded for a strictly vertical cone.

The soil profile at the Myeongji site is similar to that at the Shinho site. The silty sand layer starts at 33 m depth, i.e., about 5 m to 15 m higher than at the Shinho site.

The pore pressure distribution at the Shinho site was measured in a piezometer station installed 12 m away from the bidirectional-cell test pile to depths of 13 m, 20 m, 27 m, and 44 m. Frequent measurements were taken from about three months before the test pile was driven through about two years after the static loading tests. The measurements show ongoing consolidation in the clay layer. As illustrated in Figure 2, the 12-m distance from the piezometer station to the test pile was sufficient for the pore pressure measurements not to be affected by the driving.

At the time of the static loading test (August 20), the excess pore pressure (measured September 13) was about 30 kPa in the

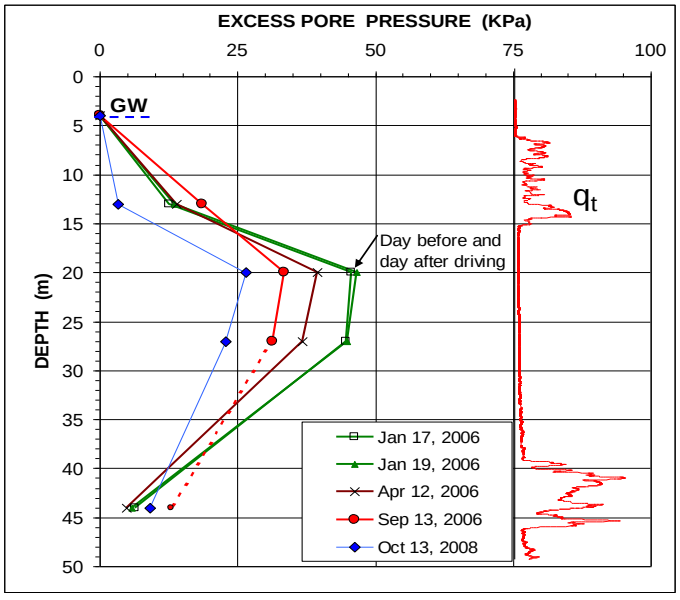

Fig. 2 Distribution of pore pressure measured about 10 m away from the Shinho bidirectional-cell test pile

clay layer. A slight excess pore pressure was also present in the silty clay layer below the clay. Significant consolidation of the soft clay layer is expected to occur after construction of the new buildings. During the seven-month set-up period between driving and testing the test piles, the ground surface settlement at the Shinho site ranged from 30 mm through 70 mm.

3. THE PHC PILE

The PHC (Pretensioned spun High strength Concrete pile) pile, a hollow cylindrical prestressed concrete pile, was developed in Japan in early 1970s, and was introduced to Korea in early 1990s. (In North America, a very similar pile is known as the ICP pile).

The PHC test pile used for the test pile is a closed-toe, 600 mm outside diameter, prestressed concrete cylinder with an 85 mm wall (total concrete cross section area is 1,375 cm^2 and the area of the central void is 1,450 cm^2), embedding twenty-four 9.2 mm rebars of steel yield 1,300 MPa (steel area is 16 cm^2, and steel area to concrete area ratio is 1.2 %) which are anchored to a donut-shaped steel plate at each segment end. The pile is cast in 5 m to 15 m long segments. The net prestress is about 8 MPa. The concrete consists of Portland cement and the concrete aggregates are crushed granite. The nominal cube strength is 80 MPa. In the field, the segments are spliced by welding the end plates together, making one splice at a time, as the pile is driven. The desired allowable load for the project piles is 2,300 kN.

The limiting axial stress of the pile in compression is determined by the combined strength of the concrete and steel. Recognizing the requirement of strain compatibility, at a strain of 0.15 % and an assumed combined modulus of 30 GPa, the limiting axial compression strength of the concrete is 45 MPa or about 6,000 kN. For a pile with the central void grouted, the equivalent theoretical pile compression strength is doubled, i.e., 12,000 kN. The limiting axial tension is determined by the steel yield of the prestressing steel rebars with disregard of the contribution of the concrete (which means that the tension is assumed to occur at the location of a crack) and is about 15 MPa over the area of the cylinder wall area, or 2,000 kN. According to Korean rules (KGS 2003), the allowable driving stress is 60 % of the concrete cube strength, i.e., about 48 MPa. The allowable driving tension according to KGS (2003) is calculated as 0.25 times the square root of the cube strength plus the net prestress, i.e., 10 MPa (1,400 kN).

The Shinho pile was instrumented with pairs of vibrating wire strain gages (Type Geokon 4911A, sister-bar gages) placed diametrically opposed at twelve levels, Levels 1 through 12: at depths of 52.1 m (3.9 m above the pile toe), 49.0 m, 44.0 m, 39.0 m, 34.0 m, 29.0 m, 24.0 m, 19.0 m, 14.0 m, 9.0 m, 4.0 m, and at ground surface, respectively. Two gage pairs (A & B and C & D) were installed at Level 12, the ground surface. The strain-gages were attached to a "ladder", which was inserted into the void of the pile after the driving. The bottom end of the "ladder" was connected to a 400-mm diameter bidirectional-cell, where a telescopic arrangement made it possible for the lower cell plate, which was flush with the pile toe, to be pushed down when the cell was activated (see below). As a final step in the construction of the pile, the central void was filled with 18 MPa cement grout over its full length above the cell. The buoyant weight of the grouted test pile was 230 kN.

The Myeongji test pile was not grouted and was instrumented by attaching electrical-resistance strain gages, Type Tokyo Sokki FCB-3-350-1-11 to 6 mm diameter, 0.8 m long rebars cast into the pile wall before placing the concrete. The gages were placed at 13 levels, Levels 1 through 13, at depths of 34.0 m (1.0 m above the pile toe), 33.0 m, 30.0 m, 27.0 m, 24.0 m, 21.0 m, 18.0 m, 15.0 m, 12.0 m, 9.0 m, 6.0 m, 3.0 m, and at ground surface.

For both test piles, a telltale arrangement provided measurements of the pile toe movements.

4. THE PILE DRIVING

The Shinho test pile was driven on January 18, 2006 using a hydraulically operated, 16-tonne ram single-acting hammer (Type Dong Kwang DKH 16), and the driving was monitored with the Pile Driving Analyzer. The driving was terminated at 56 m depth, when the penetration resistance indicated that the pile toe was encountering the very dense sand and gravel layer below the silty clay zone. The penetration per blow decreased for each blow, and the CAPWAP analysis for the last blow indicates that an equivalent PRES value of 250 blows/metre or 6 blows/25 mm. The pile central void was grouted on January 21, three days after the driving.

The dynamic measurements showed that maximum compression and tension were about 35 MPa and 5 MPa, i.e., about 70 % and 50 % of the allowable values according to KGS (2003). Two CAPWAP analyses were carried out on the blow records, one on a blow record from 43 m depth and one on the records of the last blow of driving (56 m depth). At the 43 m depth, the CAPWAP-determined capacity was 2,500 kN. At end of driving, the total capacity was 4,390 kN with mobilized shaft and toe resistances of 1,980 kN and 2,410 kN, respectively. The maximum CAPWAP-determined toe movement for the blow was 9.1 mm. The toe resistance imposed by the hammer impact is considered not fully mobilized. It was anticipated that shaft and toe resistances would both increase due to setup, and it was decided to wait for seven months before carrying out the static loading tests.

On October 18, 2005, the Myeongji test pile was driven to a depth of 35 m, approximately 2 m into the silty sand layer and to a final penetration resistance of 4 mm/blow (6 bl/25mm). The pile was driven with the same hammer as used later to drive the Shinho pile. The CAPWAP determined capacity for the last blow was 3,215 kN and the shaft and toe resistances were 765 kN and 2,450 kN, respectively. (The CAPWAP-determined toe movement was 11.6 mm).

5. TESTING PROGRAMME

5.1 Setup period

It was expected that residual load would develop in the piles from the reconsolidation after the driving and the ongoing general consolidation at the site. Therefore, the strain gages of both piles were monitored throughout the set-up period to provide measurements on the expected gradual build-up of residual load.

5.2 Myeongji Pile

The static loading test on the Myeongji pile was by means of a conventional head-down test applying load increments of 200 kN every 15 minutes until the ultimate resistance was reached, whereupon the pile was to be unloaded in decrements of 300 kN every 5 minutes. The pile was loaded by increasing the pressure in two hydraulic jacks placed on the pile head and

jacking against a beam held down by sixteen anchor piles. The load was determined by separate load cells. The conventional head-down static loading test carried out on the Myeongji test pile showed that its capacity, shaft plus toe resistances, was larger than the pile structural strength. The pile failed structurally, when the applied load was 6,500 kN, before the shaft resistance was fully mobilized in the lower portion of the pile. Note, the central void of the Myeongji pile was not grouted.

5.3 Shinho Pile, Stage 1 (Bidirectional-cell Test)

To address this problem of the structural strength being smaller than the pile capacity, potentially also after grouting the central void, the Shinho test pile was equipped with a cell at the toe, and, as the first stage of the static loading test, the cell was engaged to move the pile toe down to create an opening at the cell, i.e., between the cell and the pile, using the shaft resistance as reaction. The testing schedule consisted of increasing the cell load in increments of 160 kN at every 5 minutes, recording all gage values every 30 seconds until either a bearing capacity, the upper limit of the cell (8,000 kN), or the expansion limit of the cell (200 mm) had been reached, at which event, the load would be reduced in decrements of about 400 kN every 5 minutes. The cell was to be kept open on completion of the unloading.

5.4 Shinho Pile, Stage 2 (Head-down Test)

The testing programme in the Stage 2 test consisted of loading the pile similarly to the head-down test on the Myeongji pile, adding 300 kN load increments at every 10 minutes and recording all gage values every 30 seconds until either the bearing capacity of the pile, the upper limit of the jack pressure, or the jack expansion limit had been reached, at which event the load would be reduced in steps of about 1,000 kN every 5 minutes. The test was to be performed with the cell draining (open), which means that the pile acted as a purely shaft bearing pile in the head-down test, and, as the total shaft resistance was smaller than the axial structural strength, the shaft capacity could be determined in the test.

6. TEST RESULTS

6.1 Set-up period and build-up of residual load

The strain gages — temperature and strain — were read immediately after the grouting of the Shinho pile. The hydration process of the cement grout gave rise to a steep increase of temperature, starting about 5 hours after the completion of the grouting and reaching a peak of about 65 °C about 15 hours after the grouting. During the following ten days, the temperature diminished at a progressively smaller rate to the ambient soil temperature. Figures 3 and 4 show the temperatures and strains, respectively, from five of the gage levels during the first 250 hours after the grouting was completed.

The temperature increase occurring during the first about 15 hours after grouting, gave rise to reduced strain values (apparent compression) of 25 με in the uppermost gages (at the ground surface) and 250 με in the gages nearest the pile toe.

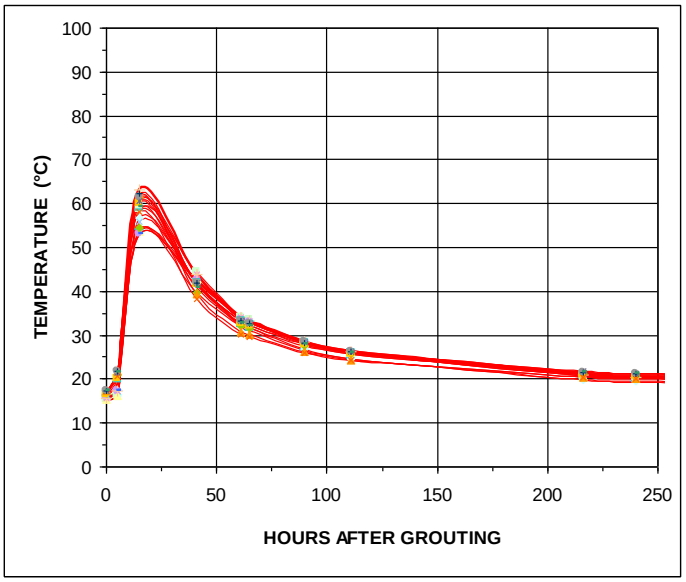

Fig. 3 Temperatures measured at the gage levels in the Shinho test pile during the first 250 hours after grouting the pile.

The reduced strains are due to the fact that the temperature elongation coefficient of the sister bar is larger than that of the hardening grout and the concrete cylinder, and, thus, full temperature elongation of the sister bars was prevented. The reverse action occurred during the subsequent cooling over the next about 100 hours, and the recorded net increase of strain values (apparent elongation) ranged from 150 με through 60 με for the gages at the ground surface to the gages at the pile toe, respectively. On the tenth day after the grouting, when the pile had cooled to the soil temperature, all gages registered a net increase of strain (apparent net tension), with a difference of about 80 με between the uppermost gages to the toe gages.

Figure 5 shows the measured strain development during 4,800 hours (200 days) after the grouting (records at intermediate gage levels are omitted for clarity). As seen, the strains recorded at gages levels at the ground surface and at 5 m depth (Nos. 12 and 11) showed little change with time after the first about 100 hours (4 days), whereas the strains from 10 m depth (No. 10) reduced slightly and the strain values measured at deeper gage levels (Nos. 9 and 2) reduced significantly.

Figure 6A shows vertical distribution of strain in the Shinho pile at different times after the grouting of the pile was completed. The strain-gage values did not drift or change during the pile driving. In contrast to the short-piece response, during the first 5 hours after the grouting, no appreciable strain change was recorded. However, the authors consider the difference to be due to that the test pile was submerged enabling it to swell from absorbing water, while the short pieces did not have access to free water until later. During the following 10 hours, the records showed increasing strain over the entire length of the pile (apparent load increase). For the next 9 days, strains decreased (apparent load decrease). Thereafter, but for the gage level at 4 m depth and at the ground surface, the strain values increased with time, i.e., suggesting that the load in the pile started to increase. The strain values continued to increase

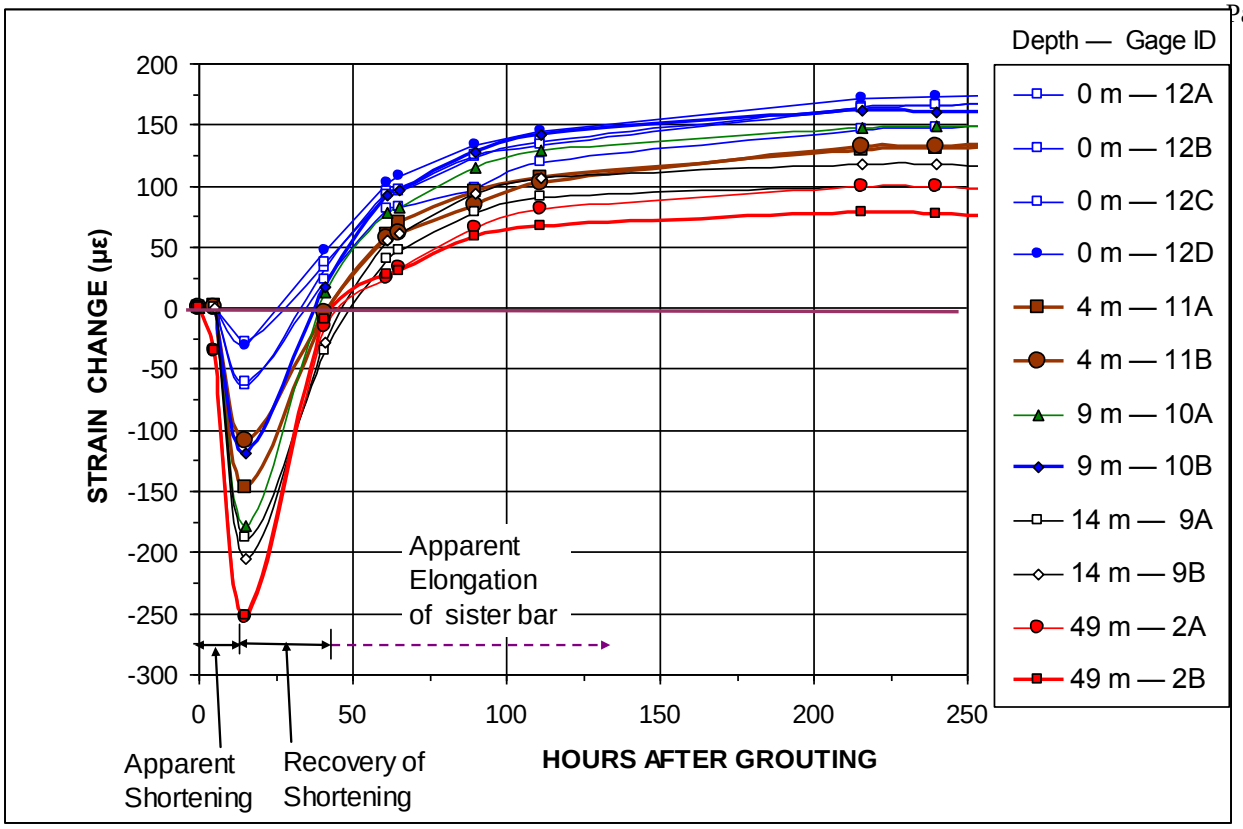

Fig. 4 Strain change measured at selected gages in the Shinho test pile during the first 250 hours after grouting the pile. The legend indicates individual gages (A or B) and gage levels (1 through 12).

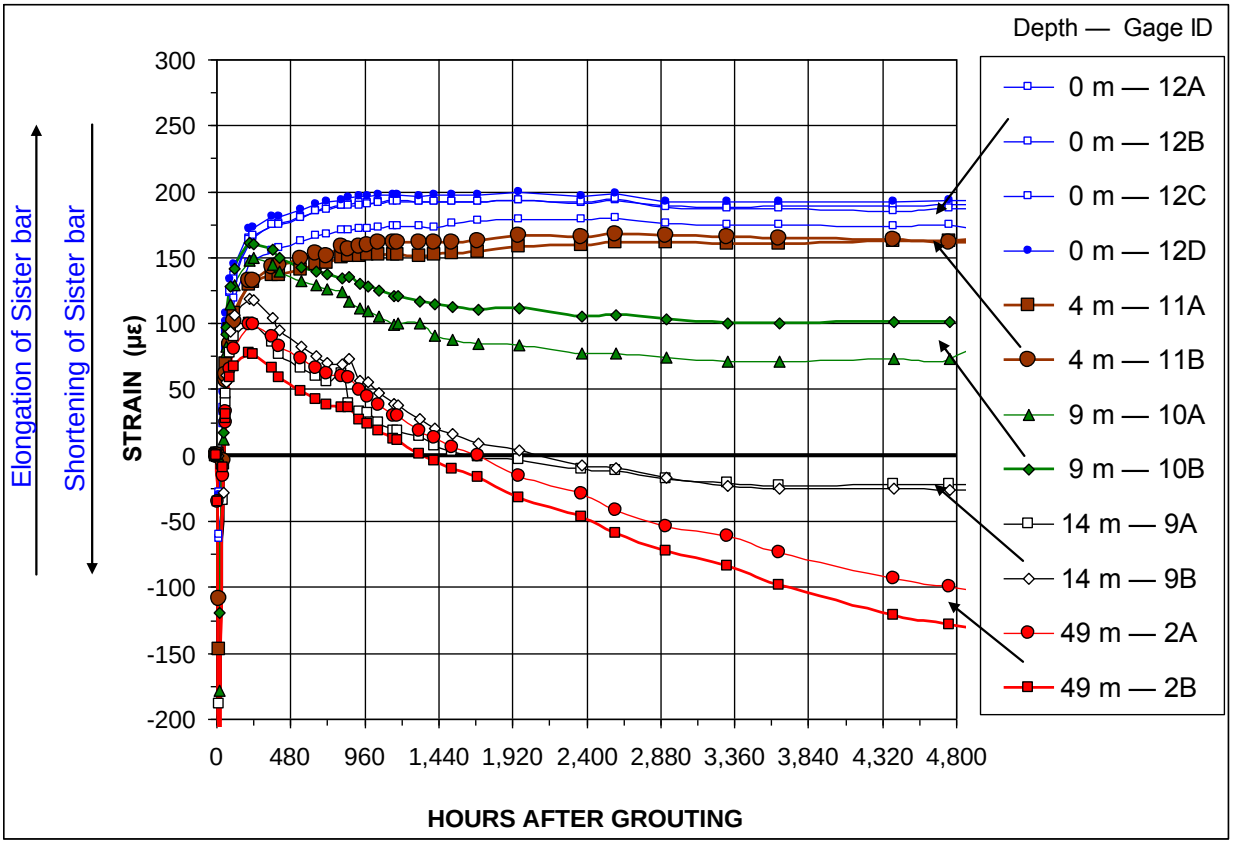

Fig. 5 Strains measured in the Shinho test pile during 200 days after grouting the pile.

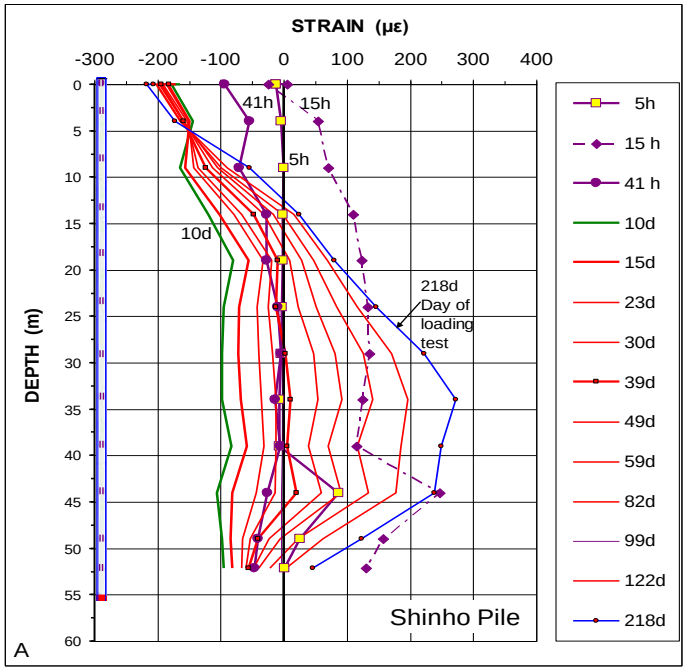

Fig. 6A Distribution of strain in Shinho pile at selected times after grouting and until day of test

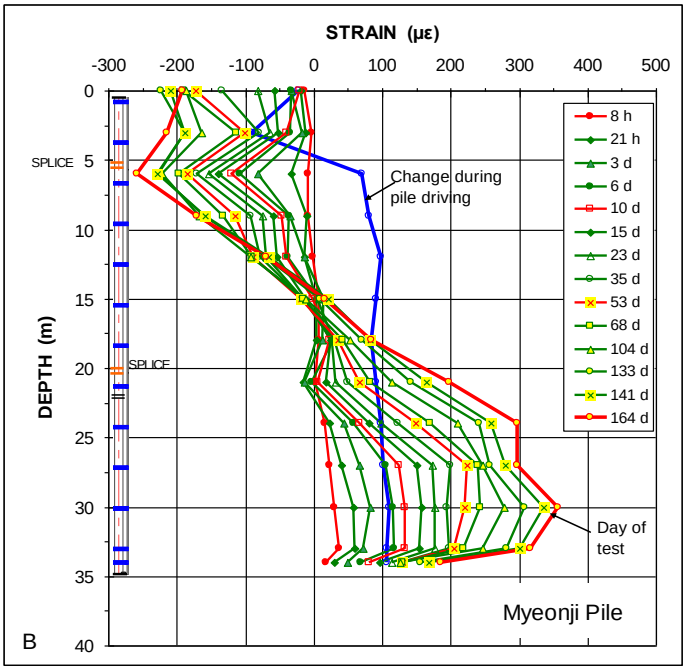

Fig. 6B Distribution of strain in Myeonji test pile during 200 days after grouting the pile

during the following 208 days (when the pile was subjected to the first static loading test, Day 218 after driving). For the portion at 4 m depth and above, the strain values instead decreased slightly after the 10th day.

Figure 6B shows the measurements of strain in the Myeongji pile. Immediately after driving, all strain gages (electrical resistance gages), except for the two nearest the ground surface indicated an about 100 με compression identified as "change during pile driving". These strains are considered due to a zero shift induced by the driving. The subsequent strain values measured during the 164-day set-up period are referenced to the values immediately after the driving, i.e., the strain gages are "zeroed" to Day 0. The strain changes during the set-up period were similar to those observed for the Shinho pile, that is, nearest the ground surface the records indicated decreasing strain, while deeper down the tendency with depth was increasing strain with time. The slope of the strain curves for the two piles is also similar.

It soon became obvious that the strain records were affected by (i) temperature increase and cooling, (ii) swelling of the pile due to its absorbing water from the soil, and, (iii) build up of residual load in the pile when the soil recovered from the driving disturbance, exacerbated by the ongoing settlement due to the fill placed on the ground. The effect of temperature (grout hydration) appears to have mostly affected the gages during the first ten days after grouting, while swelling and build-up of residual strains dominated after the tenth day. For the gage levels close to the ground surface, Gage Levels 12 and 11, no such build-up of residual load occurred.

To study the development more in detail and to separate the effects of the grout hydration and absorption of water from the build-up of residual load, a laboratory study was instigated. The laboratory study consisted of constructing two short pile pieces free-standing above ground. One piece was identical to the cylinder pile, and the other was a same diameter pile piece cast inside a temporary casing removed after the concrete had cured, serving as reference to a conventional bored pile. The study first measured temperature and strain during the hydration process and the following about 200 days. Then, a casing was placed around each pile piece and the annulus between the casing and the pile piece was filled with water. The effect of submerging of the pile pieces and the subsequent swelling due to absorption of water was measured for the following 500 days (until 700 days after the start of the study). The details and full results of this "laboratory" study are reported in a separate paper (Fellenius et al. 2009).

In summary, on grouting the short-pieces, over the first 15 hours, the temperature rose to about 85 °C and then cooled back to ambient temperature over the next about 5 days. As the temperature rose, the strain-gage records indicated an apparent 200 με shortening of the sister-bar gages. During the subsequent about 10 days of cooling, about 150 με of the shortening was recovered, leaving a net apparent shortening of 50 με. Qualitatively, the response was very similar to that observed for the uppermost two gage levels in the Shinho test pile. The strain values in the test pile show an apparent net elongation of about 100 με, as opposed to the 50 με net apparent shortening of the short piece sister bars. The authors consider the difference to be due to that the test pile was submerged enabling it to swell from absorbing water, while the short pieces did not have access to free water until later.

Beyond the first ten days through 200 days followed an additional apparent 50 με shortening of the short pieces, resulting in a net apparent shortening of about 100 με on Day 200.

The submerging of the short-pieces on Day 200 caused them to swell, which was observed as elongation of the sister bars. The swelling was rapid during the first about 10 days and amounted to about 80 με to 100 με. When correcting the records for the influence of changing ambient temperature (as described by Fellenius et al. 2009), the effect of the swelling alone could be determined for the cylinder pile as a linear trend amounting to 2 με elongation per month. (The bored pile piece, which is not restrained by the concrete cylinder, showed a linear trend of 6 με/month). For a cylinder piece submerged from the first day, assuming that the observations can be superimposed, the net strain from heating and cooling plus absorption of water over the first ten days would be about 100 με to 150 με of apparent elongation. The swelling over the following 200 days would amount to about 10 με to 15 με of apparent elongation.

It is important to realize that the change of strain values caused by the grout hydration process and absorption of water is an internal process that is practically independent of outside forces on the pile, such as residual load and imposed test load (no outside forces influenced the short pieces test). Therefore, a sister-bar recorded strain decrease due to the internal hydration process that indicates an apparent compression is associated with a corresponding apparent tension of the concrete and grout, and vice versa. It would of course have been desirable to measure also the strain changes in the concrete, but no such gages were employed. In contrast to the changes due to the internal processes, outside forces cause strain changes measured by the gages that are equal in rebars (sister bars) and concrete. The key to the analysis of the strain gage response to the applied test loads is, first, to eliminate from the records strain values that are due to internal process and, second, to separate strains due to residual load from those caused by the imposed test load.

6.2 Load-Movements, Shinho Pile, Stage 1

The Shinho test was started 218 days after the pile had been driven and grouted. The recorded load-movements of Stage 1, the bidirectional-cell test, are shown in Figure 7. The downward movement was negligible until the applied load was about 1,200 kN, which load is considered to represent the residual load at the pile toe (the pile buoyant weight is 230 kN). At the 4,430 kN maximum cell load for the first load cycle, the downward and upward movements were only 2.5 mm, and 3.0 mm, respectively.

When increasing the cell load from 4,270 kN to 4,430 kN, the downward movement increased from 2.4 mm to 5.5 mm followed within a minute by an additional 2.5 mm movement to 8.0 mm gross movement, while the pressure in the cell reduced. As this indicated that something was amiss with the test, the load was immediately released to zero in accordance with the scheduled unloading procedure. The 1st cycle downward and upward net movements after completed unloading were 6.0 mm and 0.5 mm, respectively.

The test started anew the next day (2nd cycle). Initially, the response was similar to that of the 1st cycle. However, beyond the 4,430 kN maximum load of Cycle 1 (i.e., maximum stress of 15.7 MPa) the downward movements increased progressively. The pile was unloaded when total downward and upward movements were about 90 mm and 6 mm, respectively. After unloading, it was found that one of the vibrating wire sister-bar gage pair at Gage Level 1, located 3 m above the cell, mal-functioned and was obviously impaired.

In contrast to the downward movement, the upward movement showed no progressively increasing value during the loading. In unloading, however, the upward movement became very uncharacteristic: increasing by 16 mm with decreasing load, as shown in Figure 8. Measurements of the pile head movement showed that it had not moved. Therefore, the 16 mm upward movement of the cell plate is due to damage in the pile at the cell level and over some unknown distance above. Moreover, the "plunging" downward response of the cell bottom plate is similarly associated with the cell and pile breaking up; it is not indicative of the test approaching a capacity value. The Stage 1 test results show that the mobilized toe resistance was at least 4,000 kN.

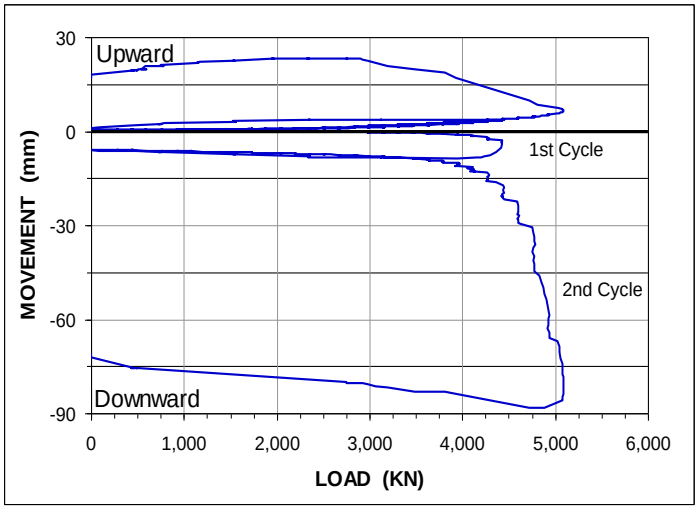

Fig. 7 Upward and downward movements of the Shinho cell plates

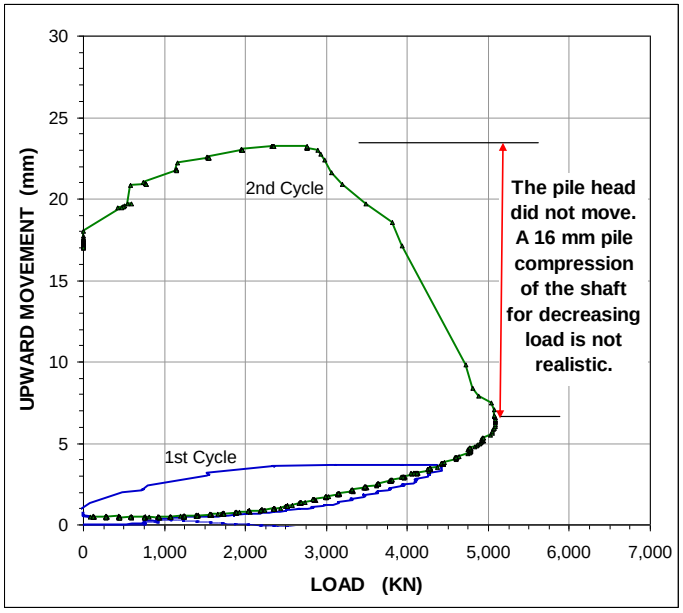

Fig. 8 Upward movements of the Shinho cell plates plotted to enlarged scale

Figure 9 shows the test-induced strain values measured at the maximum cell loads (4,430 kN and 5,070 kN, respectively) applied at the pile toe in the two cycles of the Shinho test. Also shown are the strains immediately after full release of the cell load after the tests, and the strains recorded immediately before starting the subsequent head-down test. The strain values are the change of strain in relation to the "zero" readings taken just before the start of the test. As shown, the cell load did not affect the strain gage readings above about 30 m depth, a distance of about 20 m above the cell. It is not likely that the cell load imposed any appreciable strain close to the pile head. Note, however, where the pile is subjected to fully mobilized negative direction forces, no appreciable change will be seen until the applied cell load exceeds the existing force.

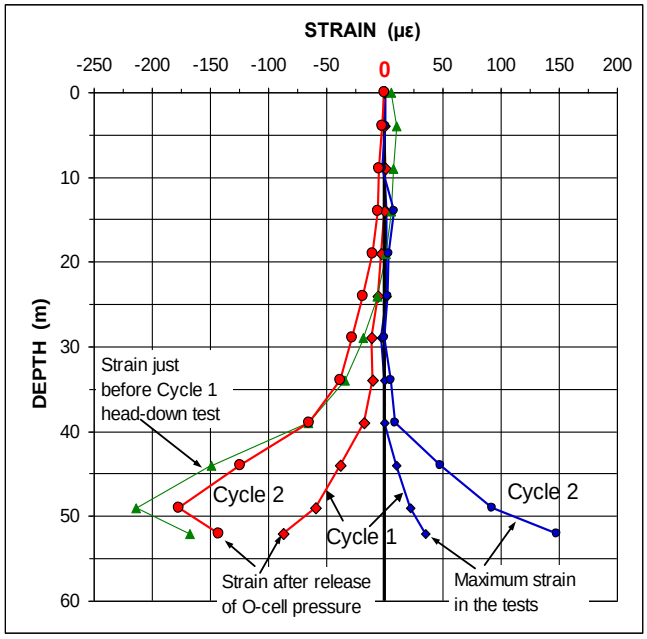

Fig. 9 Test-induced change of strain values measured at the maximum Shinho bidirectional-cell loads.

In unloading the cell, the separation of the cell plates created an about 100 mm wide axial gap, which allowed the spring effect of the locked-in stress in the pile to elongate the lower portion of the pile as evidenced by the negative strain values shown in the figure. The values are not negative in the absolute sense, but indicate the release of a portion of the residual load in the pile. Right at the pile toe, the release of the residual load is total.

The test-induced strains are small and the shaft resistance at the strain-gage levels is not fully mobilized, which precludes evaluation of the modulus of the pile material, etc. This will be addressed using the results of Stage 2, the head-down test.

6.3 Load-Movement, Shinho Pile, Stage 2 (Head-down Test)

The Shinho head-down test was carried out four days after the bidirectional-cell test. Figure 10A shows the recorded pile head load-movement. When the applied load was 8,350 kN and increasing to the next load, 8,650 kN, it was noticed that one of the jacks had sprung a leak. During the about ten minutes spent investigating whether the leak could be fixed, the load dropped to 8,135 kN. Fixing the leak showed to be not possible and the pile was unloaded. After repair of the jack, the test was restarted the next day. At the applied load of 8,900 kN, when attempting to add the next 300 kN increment to 9,200 kN and to hold this load, large increased movements occurred, making clear that the pile capacity had been surpassed. The pile was therefore unloaded. The figure also shows the recorded pile toe movement, maximum 45 mm, which closed part of the 100 mm gap created in Stage 1. The load-movement curves of the two cycles of loading have been connected with a dashed line to suggest the curves had the unloading not taken place.

6.4 Load-Movement, Myeongji Pile (Head-down Test)

The Myeongji head-down test was carried out 164 days after the pile had been driven. Figure 10B shows the load-movement curves of the pile head and pile toe. The measured shortening of the pile is also shown. When the applied load was 6,400 kN (i.e., 47 MPa over the cross section) the pile head suddenly burst. The pile structural strength (nominally 6,000 kN) had been exceeded, and the test was over. When the pile head burst, the strains induced in the pile at the two gage pairs at Gage Level 13 were 1,200 με and 1,300 με.

6.5 Strain Measurements, Shinho Pile, Stage 2 (Head-down Test)

Figures 11A and 11B show the load-strain values recorded during the 1st and 2nd cycles of the Shinho head-down test. The reference strains — the "zero" readings — are the readings taken immediately before the start of Stage 1, the bidirectional-cell test. The strain development is smooth, indicating good data, as would be expected from a pile with a well-defined cross section. The strain data of Gage Levels 12 and 11 plot very near each other and show a slope of about 25 GPa. The slope of the gage levels located deeper in the pile also appear approximately straight, but they are progressively steeper indicating that the shaft resistance is not fully mobilized but for the very last load increments.

Determining the loads represented by the strain values requires knowledge of the pile material 'elastic' modulus. Recognizing that the modulus of concrete is not a constant, but reduces with increasing strain, the modulus to use is the secant modulus. The best method for determining the secant modulus is from a "tangent-modulus" plot (Fellenius 1989, 2009). Figures 12A and 12B show the tangent modulus plot from Cycles 1 and 2, respectively, from Gage Levels 12 through 8. The lines and equations for linear regression of the data from Gage Levels 12 and 11 are indicated in both figures and show a close similarity. The average equation for the secant E-modulus, E_s, is 29.0 – 0.006 με GPa. That is, at small (zero) strains, the E_s-modulus is 29.0 GPa and at a strain of 1,000 με, the E_s-modulus has reduced to 23.0 GPa. The average modulus is 25.0 GPa. For both Cycles 1 and 2, the deeper located gage levels were affected by changing shaft resistance (but for the last increment; see information in reference to Figure 16) and, therefore, the curves do not develop a tangent-modulus line. For Cycle 2, the data are also affected from being reloading values as opposed to virgin loading.

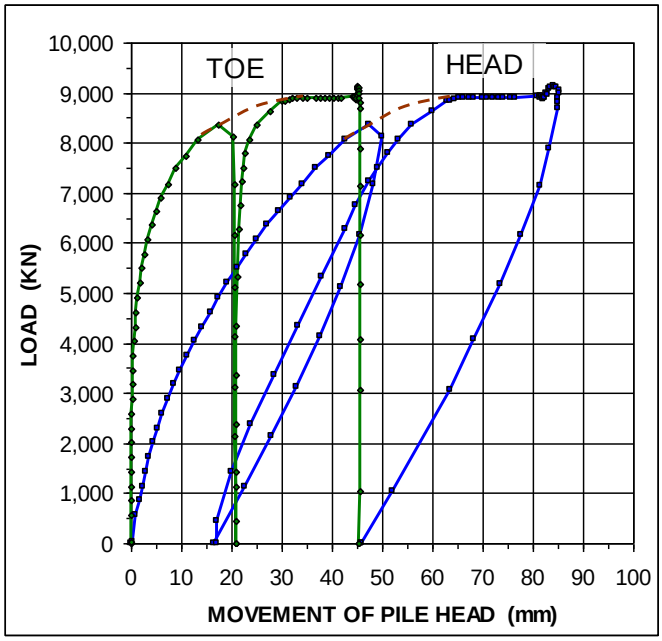

Fig. 10A Pile head and pile toe load-movements measured in the Shinho head-down test

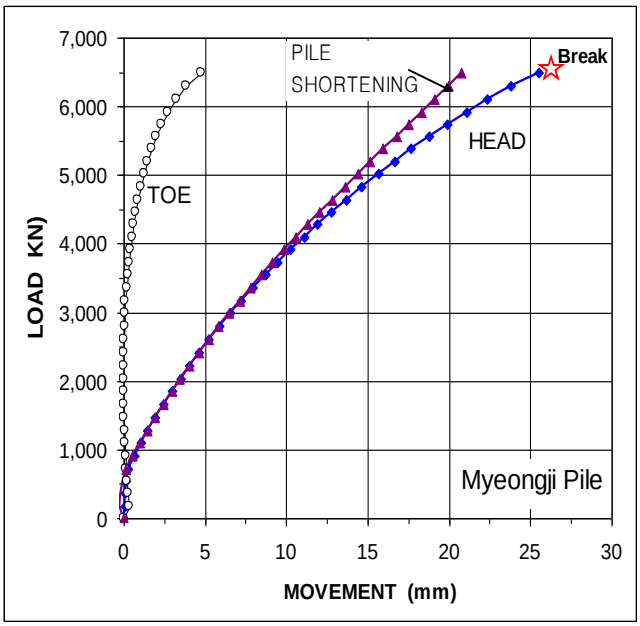

Fig. 10B Pile head and pile toe load-movements measured in the Myeongji head-down test

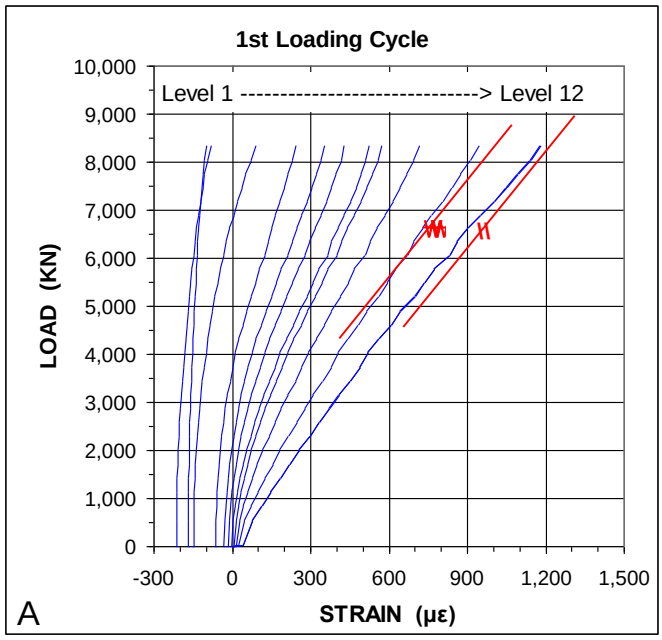

Fig. 11A Load-strain recorded in Shinho Pile Cycle 1 gages

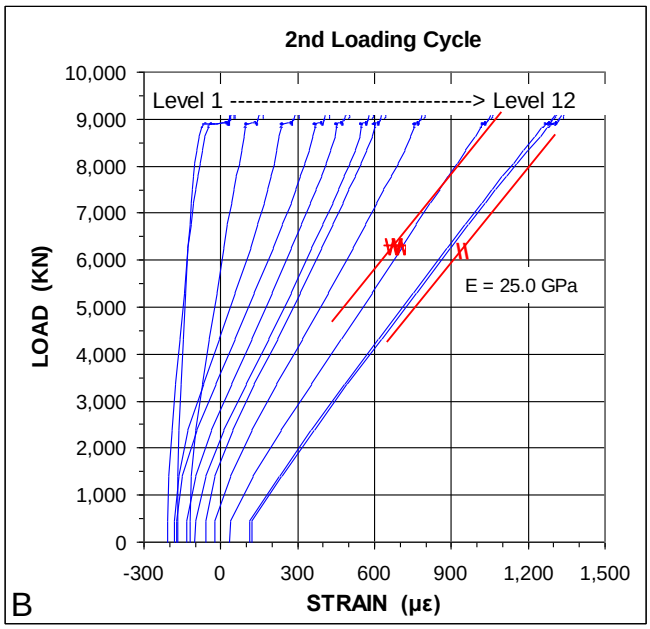

Fig. 11B Load-strain recorded in Shinho Pile Cycle 2 gages

Figures 13A and 13B show the load distributions for the applied loads for the head-down Cycle 1 and 2 head-down tests. The distributions are determined from the measured strains by applying the secant modulus to the induced strain values (i.e., the reference "zero" strain is the initial reading immediately before the bidirectional-cell test). Thus, the loads shown do not include the loads present in the pile at the start of the test — the residual load in the test pile. After unloading the test pile, the values of net strain indicate negative loads below 10 m depth, which suggests that that the test released some of the residual load inthe pile. However, the fact that the "after unloading" curves from Cycle 2 are almost the same as that from Cycle 1 indicates that no additional such release occurred in Cycle 2. Actually,Cycle 2 re-introduced a net compression strain in the lower three gage levels. The "after unloading" net compression indicated above 10 m depth is interpreted to be caused by that the release (pile lengthening) below this depth made the pile "spring" back upward, resisted by shaft shear, which caused an increase of load (strain) in the portion above 10 m depth. For reference, the unloading load distribution curves from the test are also included.

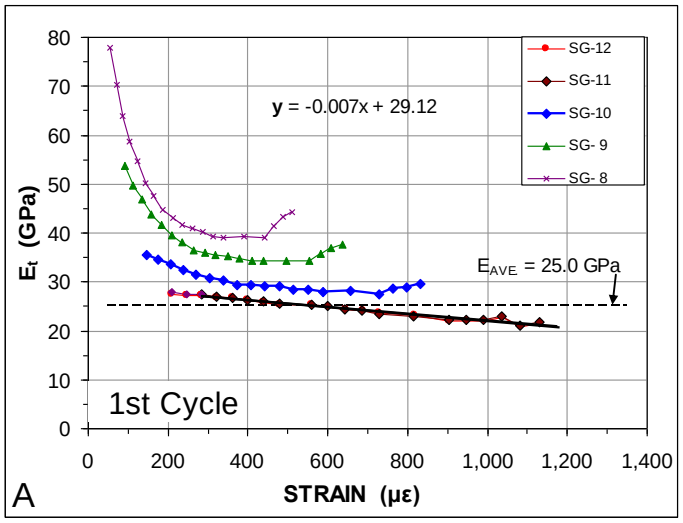

Fig. 12A Tangent modulus graph from measurements of load and strain in the Shinho pile, Stage 2, Cycle 1.

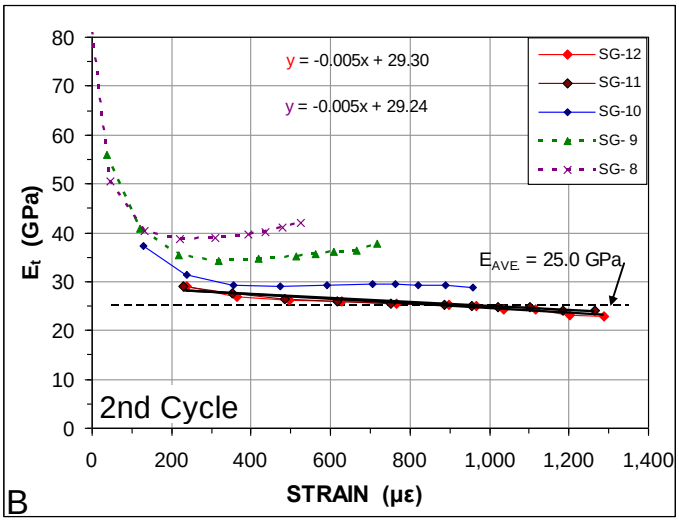

Fig. 12B Tangent modulus graph from measurements of load and strain in the Shinho pile, Stage 2, Cycle 2.

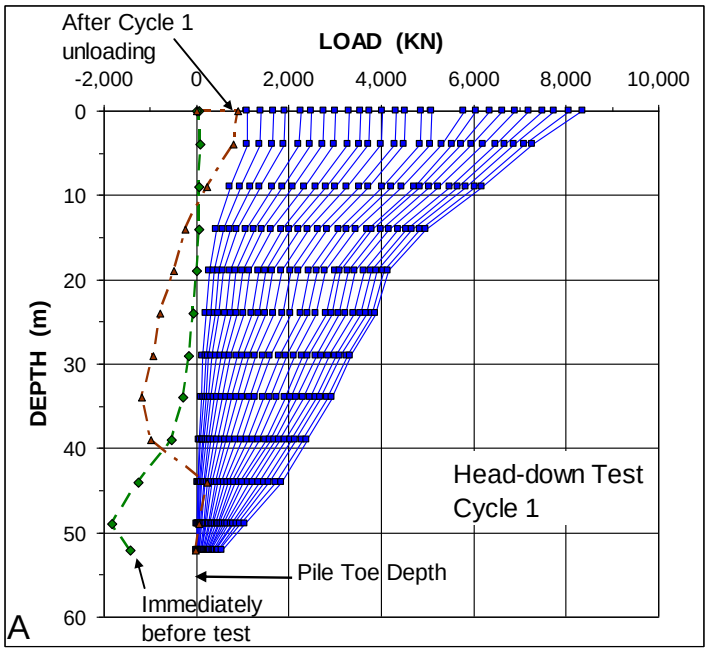

Fig. 13A Distribution of load in Shinho, Stage 2, Cycle 1 from the imposed strains uncorrected for residual load. Also shown are the load distributions determined from the strains after unloading the pile after the bidirectional test Cycle 2 and after the Head-down test Cycle 1.

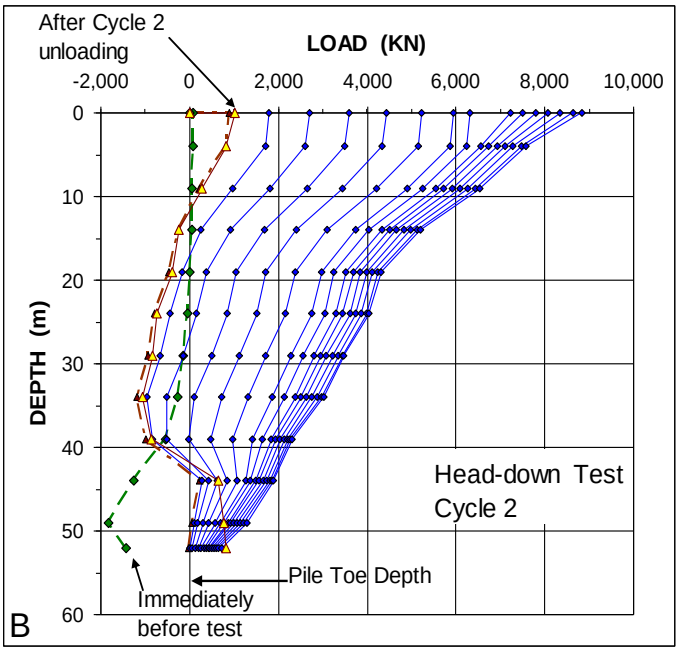

Fig. 13B Distribution of load in Shinho, Stage 2, Cycle 2 from the imposed strains uncorrected for residual load. Also shown are the load distributions determined from the strains after unloading the pile after the bidirectional-cell test Cycle 2 and after the Head-down test Cycles 1 and 2.

Figure 14 shows the measured shortening of the Shinho pile plotted versus the pile toe movement. When the shaft resistance had become fully mobilized, the pile moved monolithically, which is an indication that the shaft resistance did not soften during continued shear movement in either cycle. The small reduction of the shortening for the last value in Cycle 1 is not due to softening, but to that the applied load was let to reduce when the source of the leak was investigated.

Fellenius (2002, 2009) presented a method for estimating the residual load distribution in a pile directly from the load distribution curve determined from the load induced in the test, i.e., from the "zero" readings. The method assumes that the residual load is built-up from fully mobilized shaft shear in the upper portion of the pile, and, therefore, the "true" shaft resistance and the residual load are both equal to half the apparent reduction of load due to shaft resistance. This

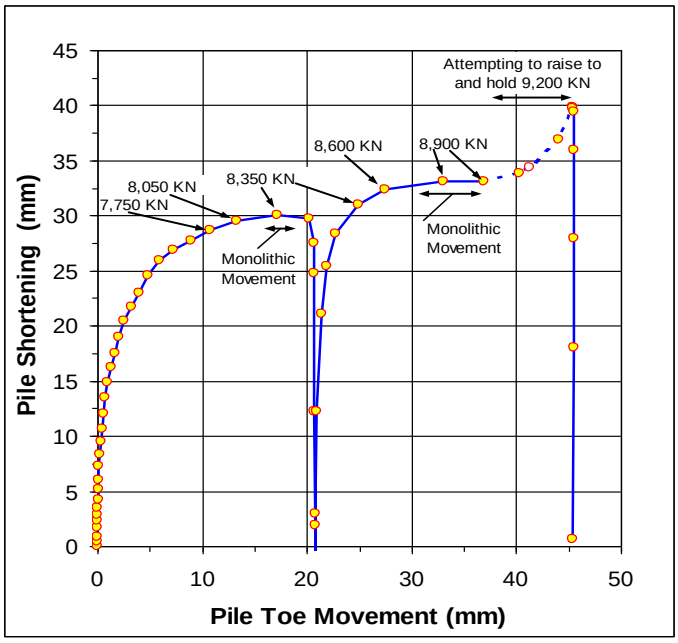

Fig. 14 Pile shortening versus pile toe movement in Shinho head-down test

assumption is valid down to where the downward-directed shear forces (negative skin friction) starts to diminish within a transition zone between the negative and positive direction of shear force along the pile. Below the transition zone, the residual shear forces are again more or less fully mobilized, now in the positive direction. An advantage for the analysis of the data from the subject test is provided by the fact that the 100 mm net opening between the cell plates of the initial test removed all residual toe load and eliminated the ability of the pile to build up toe resistance.

Figure 15A shows the measured distributions (Curve A) for the 8,350 kN maximum load applied to the pile head in the Cycle 1 test on the Shinho pile. Curve B is the distribution of residual load calculated as half the apparent reduction of load due to shaft resistance shown by Curve A from the pile head to the pile toe. This curve is the first step in determining the distribution of residual load present in the pile at the start of the test. It is assumed that shaft resistance is fully mobilized and equal in negative and positive directions of shear. This assumption is considered valid down to where the unit shear force starts to reduce and to change from negative direction to positive direction. This point is the end of fully mobilized residual load, and is marked "Residual shear fully mobilized". Whether this point lies at the indicated depth of 34 m, a bit higher up in the clay layer, or a bit lower (say, at the interface of the clay and sand layer at about 39 m depth) is a judgment call here aided by the fact that neither residual load nor toe resistance exist at the pile toe. A further aid is found from reference to the soil layering indicated in the cone sounding diagram shown to the side of the diagram. The plotting of the continued residual load from below the neutral plane, where its magnitude is reduced due to positive shaft resistance, is also governed by judgment, aided from the condition that it cannot show a larger shaft resistance (i.e., have a flatter slope) than the positive shaft resistance indicated by Curve D. The latter is simply determined as Curve A values plus Curve C values, and it is the "true" distribution of load in the pile.

Also shown in Figure 15A is a Curve E, which is the "true" resistance curve (D) fitted to an effective stress calculation resulting in the ß-coefficients indicated in the column to the right of the graph. The density values are those given in the site condition section and the pore pressure distribution incorporates a 30 kPa excess pore pressure for the silty clay between 15 m through 40 m depth. The simple array of ß-coefficients shown makes the two curves plot on top of each other.

Figure 15B shows the identical calculations for the 7,750 kN load applied to the pile two increments earlier in the test. Curve C down to 34 m depth is determined from Curve A, while below 34 m depth the values are identical to those of Figure 15A. Curve C from Figure 15 A is added to the graph and the difference between the two C-curves demonstrates that the method of analysis is not exact because, theoretically, the two curves should have been equal, as the same full shaft resistance can be assumed to have been mobilized along the upper portion of the pile also for the 7,750 kN load.

Figure 15C shows the calculations for the 8,350 kN load applied to the pile in Cycle 2. Again, Curve C down to 34 m depth is determined from Curve A, while below 34 m depth the values are identical to those of Figure 15A. The calculated distributions of residual load and shaft resistance are very similar to those shown in Figure 15A. Figure 15D shows the calculations for the 8,900 kN load and demonstrates, as in Cycle 1, that the calculated residual loads for the two cases are very similar albeit not exact. The difference is slight and the four analyses shown in Figure 15A through 15D can be taken as resulting in the same distributions of residual load and shaft resistance for the test pile.

Figure 16 compares the residual loads with the loads calculated applying the same secant modulus relation to all the measured strains from the Cycle 1 of Stage 1 (bidirectional-cell test), through Cycle 2 of Stage 2 (head-down test). Curve C in the figure is the residual load distribution evaluated from Cycle 1. Curve E is the load distribution calculated from the strains measured after unloading, which is the release of residual load due to the net opening of the cell (loads are shown negative). Combining Curves C and E (adding their absolute values) results in Curve F, the residual load in the pile immediately before the start of Cycle 1.

For reference, Figure 16 also shows Curve G, which is the load distribution calculated from the change of strain developed after the grouting of the Shinho pile, taking the strain at Day 10 after the grouting as zero reference. The strains after Day 10 are considered dominated by shear forces developing between the pile and the soil. Curve H is the distribution of load calculated from the strains developing from the day of the grouting until Day 10, which strains are strongly affected by the internal processes (temperature changes in the grout and swelling). It is tempting to add Curves G and H and subtract Curve F to arrive at the effect of the internal processes during the first ten days after the grouting of the pile. However, this would be little more than a conjecture. Note also that the residual load—magnitude unknown—that must have developed in the pile during the three days between driving and grouting the pile is

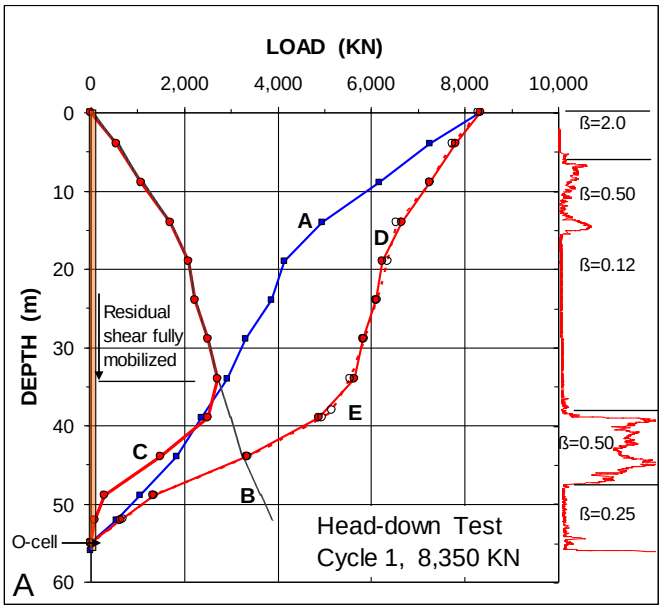

Fig. 15A Construction of the Shinho residual load. Cycle 1 for applied 8,350 kN applied load

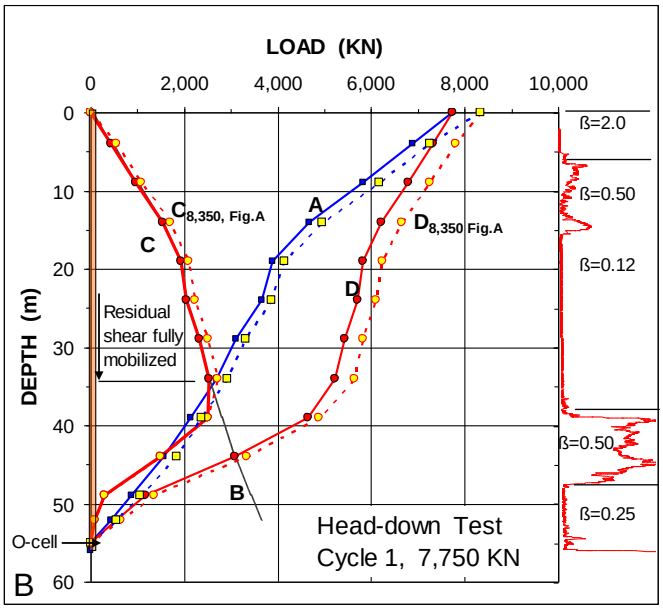

Fig. 15B Construction of the Shinho residual load. Cycle 1 for applied 7,750 kN applied load

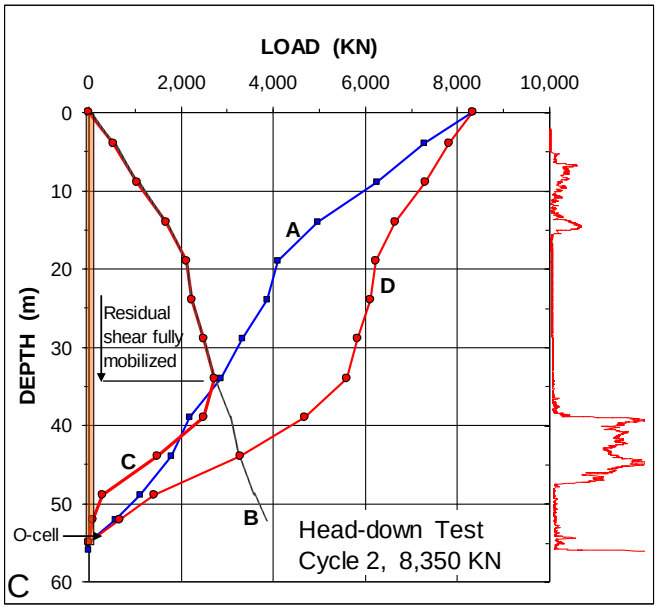

Fig. 15C Construction of the Shinho residual load. Cycle 2 for applied 8,350 kN applied load

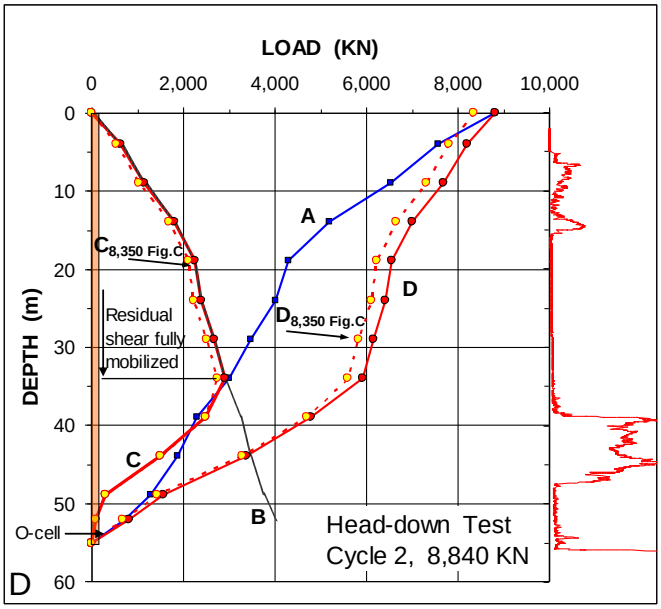

Fig. 15D Construction of the Shinho residual load. Cycle 2 for applied 8,840 kN applied load

not included in Curve H. The main use of the CPTu sounding in this paper is as reference to the soil layering. In general, however, the results of CPTU soundings are also considered particularly suitable for calculation of capacity and resistance distribution of piles. The shaft resistance determined by the CPTU method proposed by Eslami and Fellenius (1997) is shown in Figure 17 together with the distribution of the "true" shaft resistance. The CPTU curve has been moved laterally to best suit the "true" resistance in order to facilitate a comparison between the "true" and the CPTU-determined shaft resistance. Down to about 50 m depth, the CPTU determined value agrees reasonably well with the "true" resistance, but below, in the sand, it is quite off. Possibly, the pile driving has densified the sand, and, although the sounding was made after the pile driving it was not close enough to the test pile to register any effect of the driving.

6.6 Myeongji Pile

The test data recorded in the loading test on the Myeongji pile were analyzed the same way as described for the Shinho pile test. The pile response to the driving in terms of tension and compression stresses was about the same as recorded for the Shinho pile. The tangent modulus method gave a secant modulus, E_s (GPa), of 39.0 - 0.003με, about 50 % larger than the value determined for the grouted Shinho pile. The load distributions for the applied loads were calculated using this

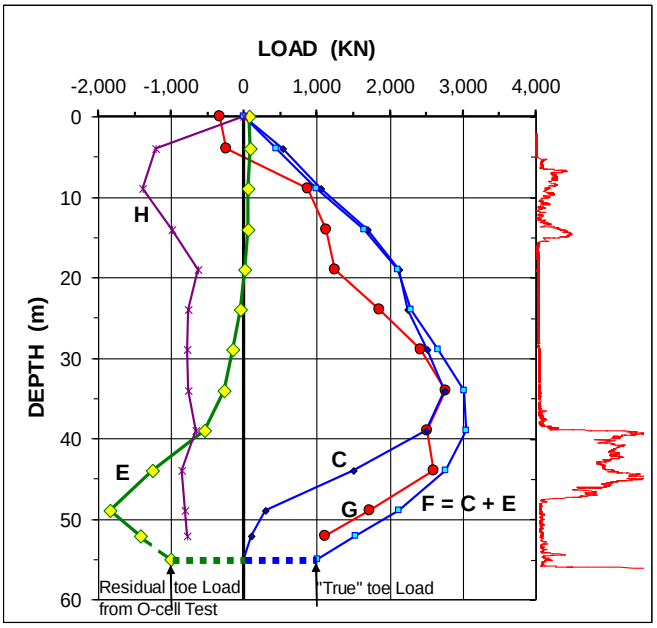

Fig. 16 Residual load (C) in the Shinho pile determined by the method proposed by Fellenius (2004, 2009) for Stage 2 test and residual load (F) for Stage 1 test on adding the release of load after unloading the Stage 1 test (bidirectional-cell test)

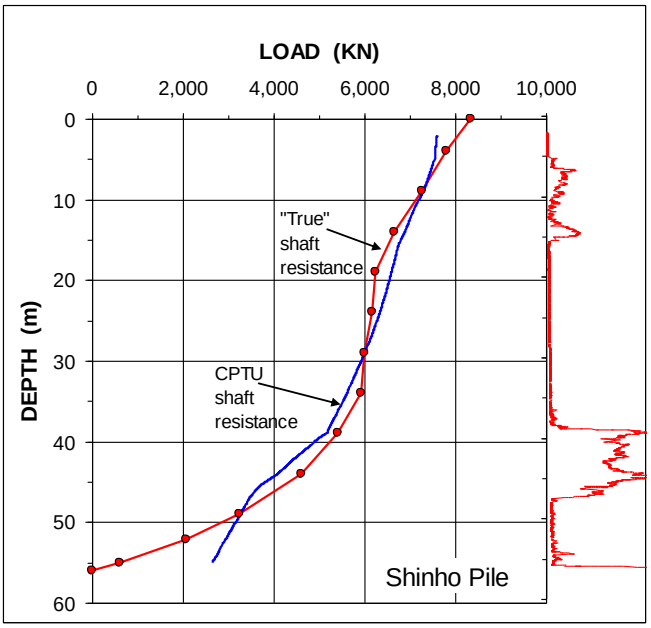

Fig. 17 "True" shaft resistance distribution (Curves A and F added) in the Shinho pile test and shaft resistance calculated from the CPTU method. The latter is offset in order to provide a better comparison to the "true" distribution

modulus and, the results are shown in Figure 18. The figure also shows the curves for residual load, the "true" resistance, and the curve matched to an effective stress analysis using the beta-coefficients shown at the side of the diagram.

The results of a CPTU sounding close to the Myeongji pile location are shown to the side of the figure. The shaft resistance curve determined by the Eslami-Fellenius method from the CPTU data is plotted next to the shaft resistance distribution. The curve has been offset to facilitate a comparison between the "true" and the CPTU-determined shaft resistance. As for the Shinho pile, the CPTU determined value agrees reasonably with the "true" resistance, but is quite off in the sand. The static cone at the Myeongji site was pushed before the static loading test was performed. Therefore, the values are unaffected by potential densification of the sand due to the pile driving.

The results from the 35 m long Myeongji pile are in all applicable aspects similar to the results of the 57 m long Shinho pile.

7. APPLICATION OF THE RESULTS TO THE DESIGN OF THE PILED FOUNDATIONS

The construction piles supporting the new buildings at the two sites will in the long-term be subjected to drag load and, potentially, also to downdrag, which has to be considered along with the design for the bearing capacity of the piles. This design approach is expressed in "the unified design method" (Fellenius 1984, 2004, 2009; Canadian Foundation Engineering Manual 2006, Fellenius and Ochoa, 2009), where the drag load—giving rise to a maximum load in the pile (at the neutral plane)—is considered with respect to the structural strength of the pile, and the settlement of the pile (downdrag) is recognized to be equal to the settlement of the soil at the neutral plane. The ongoing

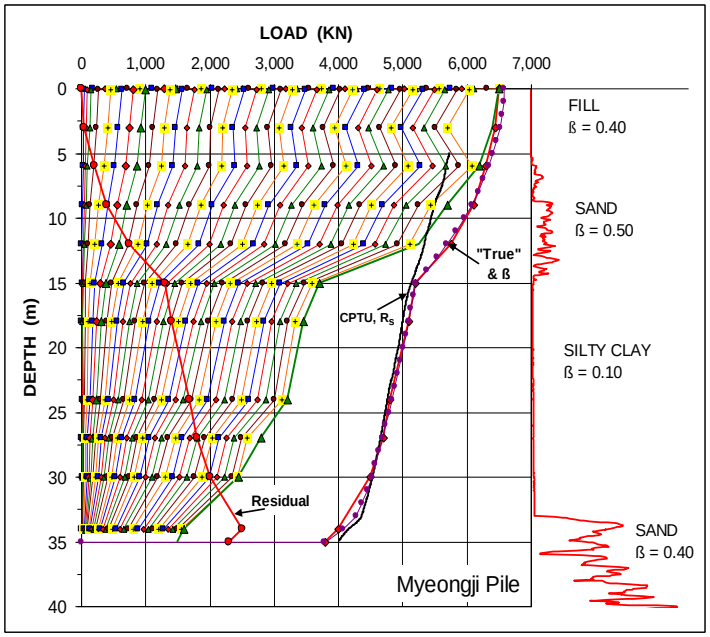

Fig. 18 Results of the head-down loading test on the Myeongji pile. Distributions of residual load, "true" resistance, resistance matched to an effective stress analysis, and shaft resistance determined from the CPTU test

consolidation of the soft clay makes it clear that it is desirable that the piles be installed such that the neutral plane does not develop any higher than a location at or slightly above the sand layer. At this depth, post-construction soil settlement will be small and, therefore, the downdrag will be small.

The pile toe penetration governs the mobilized pile toe resistance, and, provided the neutral plane lies where the long-term soil settlement is small, the long-term pile toe penetration into the dense sand layer is small, too. A conservative estimate is that the toe resistance is 4,000 kN. These conditions establish the location of the neutral plane (force equilibrium as well as settlement equilibrium) and the magnitude of the maximum load in the pile.

Based on the test results, the load distribution can be determined for a construction pile at the Shinho site similar to the test pile. Figure 19 shows the distribution for a 55 m long pile subjected to a sustained load, Q_d, equal to the mentioned allowable load of 2,300 kN. As shown, the load in the pile will increase due to negative skin friction down to the lower boundary of the soft clay at about 39 m depth, stay more or less constant within a relatively short transition zone, and, then, reduce to an estimated about 4,000 kN toe resistance. The maximum load in the pile will be about 6,000 kN and the drag load will amount to about 4,000 kN. This maximum load is close to the structural strength of the cylinder pile. Therefore, to ensure structural integrity and adequate structural strength, the lower lengths of the pile, about 30 m total, will have to be grouted to increase the axial structural strength. The soil settlement at the neutral plane is estimated to be no more than a few millimetre. Therefore, the long-term settlement of the foundations will consist of mostly load-transfer movement, which is about equal to the downdrag and 'elastic' compression of the pile due to the imposed load, in all less than about 10 mm. The pile capacity does not govern the design, because the pile capacity (for a mobilized toe resistance of 4,000 kN) is approximately 12,300 kN, which is several times the allowable load.

Were the piles to be installed at the Shinho site to a capacity just adequate for the desired allowable load, they could be much shorter, say about 40 m. The maximum load for that shorter pile could well show to be within acceptable limit for the structural strength without grouting the pile central void. However, the neutral plane would be located up in the soft clay and the piled foundation would experience unacceptably large long-term settlement.

Figure 20 shows the similar curves for the shorter pile, the Myeongji pile. Again, total capacity of the pile will not be an issue for the design. Settlement (downdrag) and axial structural strength might be, however. Provided that the pile driving develops a good toe resistance in the sand layer, the neutral plane will be at or close to the sand layer and downdrag will be minimal. For a pile of the length shown, the pile structural strength is adequate for resisting the maximum load in the pile without grouting the pile central void. However, where the piles become longer because the soft clay layer is thicker, the design will consider upgrading the structural strength of the pile by, for example, grouting the pile void.

At both sites, the long-term load distribution and location of the neutral plane is governed by the magnitude of the pile toe resistance, which is a function of the pile toe penetration into the sand layer. The penetration is about equal to the settlement at the neutral plane. The analysis of the strain gage records provide the pile toe resistance, which together with the pile toe movement measured for the Myeongji pile gives the relation for

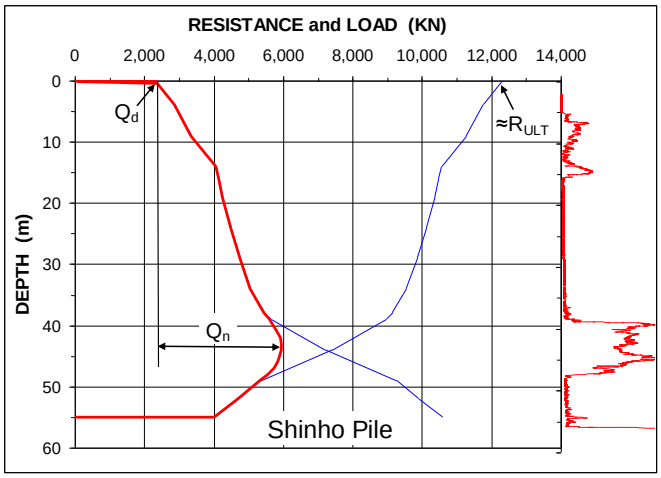

Fig. 19 Long-term resistance and load distributions for a construction pile at the Shinho site, a pile similar to the test pile at the Shinho site

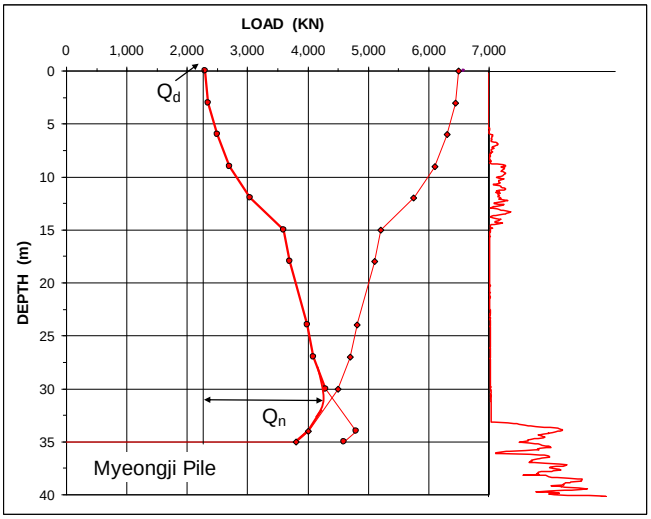

Fig. 20 Long-term resistance and load distributions for a construction pile at the Myeongji site similar to the test pile at the Myeongji site

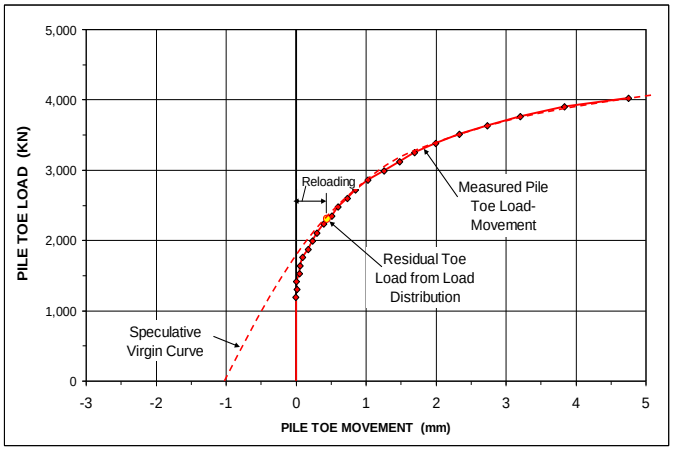

Fig. 21 Myeongji pile. Toe resistance evaluated from the strain gages and measured pile toe movement plus speculative virgin curve

the pile toe load-movement, as shown in Figure 21. The figure also shows the residual pile toe load established in the analysis. Thus, the curve consists of a reloading part and a virgin part. An approximate — somewhat speculative — virgin curve has been added to the figure to indicate a possible load-movement response had there been no residual toe load. However, for these piles, the driving alone will induce a residual toe load and due to the build-up of residual load along the pile shaft after driving, the toe residual load at the pile toe will increase. Therefore, already a small settlement at the neutral plane will result in a significant increase of the pile toe load and, probably a lowering of the neutral plane. Thus, the pile testing programme has shown that (1) the long-term settlement of the piles is expected to be small, and (2) the key design aspects for this site are the maximum load in the pile and the pile structural strength.

8. SUMMARY OF FINDINGS AND CONCLUSIONS

The test objectives were reached and the results can be summarized in the following points.

1. The values of measured maximum compression and tension during the driving were 70 % and 50 %, respectively, of the allowable values, and the pile driving was shown not to overstress the pile.

2. The build-up of residual load in the Shinho pile started immediately after the driving and was still continuing seven months later, when the static loading tests were carried out.

3. The strain records showed an about 50 με to 200 με reduction in the sister-bar strain-gage values during the first about 20 hours after driving. During the next about ten days, the reduction was recovered, whereafter the strain values again indicated a slow increase of strain values continuing during the seven-month wait until the static loading test was carried out. During the ten first days, the strain changes were mostly due to internal processes caused by temperature effects during the hydration of the grout and swelling of the grout and concrete by absorption of water from the ground. Thereafter the increase of strain was caused by increased load in the pile, due to the soil set-up and ongoing consolidation of the thick soft clay layer at the site, which involved interaction with external shear forces along the pile.

4. A special laboratory study of strain changes due to hydration, only, and to swelling, only, without influence of residual load, showed that the influence on the measurement due to hydration and swelling was a significant portion of the total strains measured in the test pile during the set-up period.

5. For a cylinder piece submerged from the first day, assuming that the observations can be superimposed, the net strain from heating and cooling plus absorption of water over the first ten days would be about 100 με to 150 με of apparent elongation. The swelling over the following 200 days would amount to about 10 με to 15 με of apparent elongation. The strains from hydration and swelling are about one third of the total strains measured during the set-up period.

6. Judging from the measurement in the test pile and the special short pieces test, for the first ten days after the driving and grouting, the strain process is dominated by hydration and swelling. Thereafter, the increase of strain is mostly due to build-up of residual load from the soil. It is not possible to determine the relative magnitude of the two influences from strain-gage records alone with acceptable degree of precision.

7. While the head-down loading test on the 35 m long Myeongji pile did mobilize the pile shaft resistance, the small portion of the maximum test load that reached the pile toe (about 2,000 kN) showed that the total capacity of the pile was not reached when the structural failure occurred. A pile of the same length strengthened by grouting the central hole would have had sufficient strength to be tested to the full static capacity. However, had the strengthened pile been longer, it would probably not have withstood the then necessary maximum test load. The combination of the bidirectional-cell test and the head-down test resolved this dilemma.

8. The bidirectional-cell test showed the Shinho pile toe resistance to be at least 4,000 kN. The test was successful in establishing a gap at the pile toe so that the pile functioned as a purely shaft bearing pile in the subsequent head-down test. The bidirectional-cell test also indicated that the residual toe load is as least 1,200 kN. The residual toe load showed to have been released after the unloading of the pile.

9. The head-down test showed the shaft resistance of the Shinho test pile to be 8,400 kN. Tangent-modulus analysis of the strain gages in both test pile established the secant pile modulus, E_s (GPa), to use in converting the strain values to load as $29 - 0.006\ \mu\varepsilon$. The average modulus was 25 GPa. The corresponding values for the Myeongji pile were similar.

10. The CAPWAP analysis for the end-of-driving impact showed a shaft resistance of about 2,000 kN for the Shinho pile. The additional shaft resistance due to set-up thus amounted to about 6,500 kN.

11. The Shinho strain-gage converted distribution of load was corrected for residual load and showed the residual load equilibrium (neutral plane) to be located between 34 m to 39 m depth. The maximum residual load in the pile was about 3,000 kN. The "true" shaft resistance distribution corrected for the residual load showed that the unit shaft resistance in the soft clay was small, corresponding to an effective stress beta-coefficient of only 0.12. In the dense silty sand, the unit shaft resistance corresponded to a beta-coefficient of 0.50.

12. The analysis of the Myeongji test results load distribution showed distributions of shaft resistance and beta-coefficients very similar to those of the Shinho pile.

13. For both test piles, the CPTU-determined shaft resistance in the soft clay agreed well with that from the tests but indicated a significantly smaller value in the sand layer. A possible reason could be that the pile driving densified the sand which caused the shaft resistance to increase.

14. Calculations of the long-term conditions for a construction pile similar to the test piles show the pile capacity to be more than adequate for the 2,300 kN allowable load. For pile longer than about 30 m, the maximum load in the pile (at the neutral plane) will approach the structural strength of the pile and grouting the pile to strengthen its axial structural strength should be considered. As the long-term settlement at the location of the neutral plane will be small, the long-term settlement of the piled foundations will be acceptable to the design.

ACkNOWLEDGEMENTS

This work was supported by a grant from the Korea Science and Engineering Foundation (KOSEF) NRL Programme funded by the Korean government (MEST; No. R0A-2008-000-20076-0), and by Young Jo Engineering & Construction Co., Ltd., Seoul. Mr. Thomas Molnit at LOADTEST Asia Pte. Ltd., Dr. M.H. Lee at PILETECH, Seoul, and post-graduate students at Dong-A University, Busan, provided valuable assistance with the field tests.

REFERENCES

Canadian Foundation Engineering Manual, CFEM, 2006. Fourth Edition. Canadian Geotechnical Society, BiTech Publishers, Vancouver, 488 p.

Chung, S.G., Giao, P.H., Kim, G.J., and Leroueil, S., 2002. Geotechnical properties of Pusan clays. Canadian. Geotechnical Journal. 39(5) 1050–1060.

Chung, S.G., Ryu, C.K., Jo, K.Y., and Huh, D.Y., (2005). Geological and geotechnical characteristics of marine clays at the Busan new port. Marine Georesources and Geotechnology, 23(3) 235-251.

Chung, S.G., Kim, G.J., Kim, M.S. and Ryu, C.K., 2007. Undrained shear strength from field vane test on Busan clay. Marine Georesources and Geotech., 25(3) 167-179.

Eslami A. and Fellenius B.H., 1997. Pile capacity by direct CPT and CPTu methods applied to 102 case histories. Canadian Geotechnical Journal 34(6) 886–904.

Fellenius, B.H., 1984. Negative skin friction and settlement of piles. Proceedings of the Second International Seminar, Pile Foundations, Nanyang Tech. Inst., Singapore, November 28-30, 12 p.

Fellenius B.H., 1989. Tangent modulus of piles determined from strain data. American Society of Civil Engineers, ASCE, Geotechnical Engineering Div., the 1989 Foundation Congress, Edited by F.H. Kulhawy, Vol. 1, pp. 500-510.

Fellenius, B.H., 2000. The O-Cell — A brief introduction to an innovative engineering tool. Väg- och Vattenbyggaren 47(4) 11-14.

Fellenius B.H., 2002. Determining the resistance distribution in piles, Part 1: Notes on of no-load reading and residual load. Part 2: Method for determining the residual load, Geotechnical News Magazine. 20(2): 35-38 and 20(3):25-29.

Fellenius, B.H., 2004. Unified design of piled foundations with emphasis on settlement analysis. Current Practice and Future Trends in Deep Foundations, Proceedings of the Geo-Institute Geo-TRANS Conference — Honoring George G. Goble, Los Angeles, July 27–30. Edited by J.A. DiMaggio and M.H. Hussein. Geotechnical Special Publication 125, pp. 253–275.

Fellenius, B.H., 2009. Basics of foundation design. Electronic Edition, https//: www.Fellenius.net, 340 p.

Fellenius, B.H., Kim, S.R. and Chung, S.G., 2009. Long-term monitoring of strain in strain-gage instrumented piles. ASCE Journal of Geotechnical and Geoenvironmental Engineering, 135(11) 1583-1595.

Fellenius, B.H. and Ochoa, M., 2009. Testing and design of a piled foundation project. A case history. Geotechnical Engineering, Journal of the Southeast Asian Geotechnical Society 40(3) 129-137.

Korean Geotechnical Society (KGS), 2003. Design guideline of structural foundations. Seoul, Korea, 296 p.

Osterberg, J. O., 1998. The Osterberg load test method for drilled shaft and driven piles. The first ten years. Great Lakes Area Geotechnical Conference. Seventh International Conference and Exhibition on Piling and Deep Foundations, Deep Foundation Institute, Vienna, Austria, June 15-17, 1998, 17 p.

SUPPLEMENTARY PILE DRIVING INFORMATION

In order to reduce length of the paper, the following three figures were removed from Section 4 of the original manuscript.

Figure A shows a plot of the pile driving log (penetration resistance, (PRES) and the distribution with depth of the hammer height-of-fall from the driving of the Shino test pile. The cone stress diagram also shown in the figure shows a good agreement between the trend of the cone stress and PRES distributions.

Figure B show the distribution of Case Method Estimate of capacity, CMS RMX with a J-factor of 0.4, as the pile was being driven. Two CAPWAP analyses were carried out on the blow records, one on a blow records from at a depth of 43 m and one on the last blow of driving. A CMS RX4 matches the CAPWAP determined capacities. At end of driving, the CAPWAP-determined capacity was 4,390 kN.

Figure C shows the distribution of resistance determined in the two CAPWAP analyses at 43 m depth and at EOID (56 m depth). The EOID CAPWAP-determined mobilized total and toe capacities were about 4,400 kN and 2,200 kN, respectively. During the seven months wait until the static loading test, the total capacity increased due to set-up to about 8,900 kN. The maximum load (just before the pile broke above the cell) was about 4,500 kN. Compare Figure C to Figures 13A and 13B (Section 6.3).

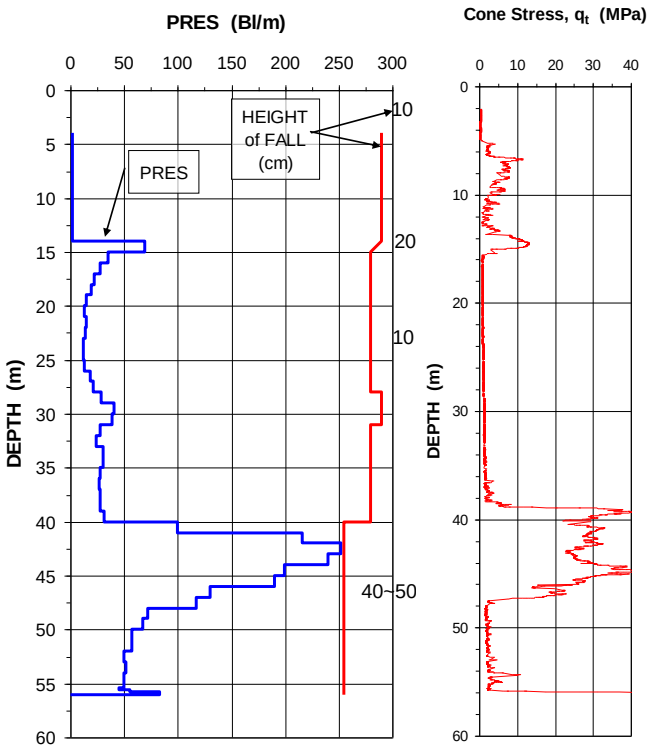

Fig. A Pile driving diagram (PRES), hammer height-of-fall, and cone stress, q_t.

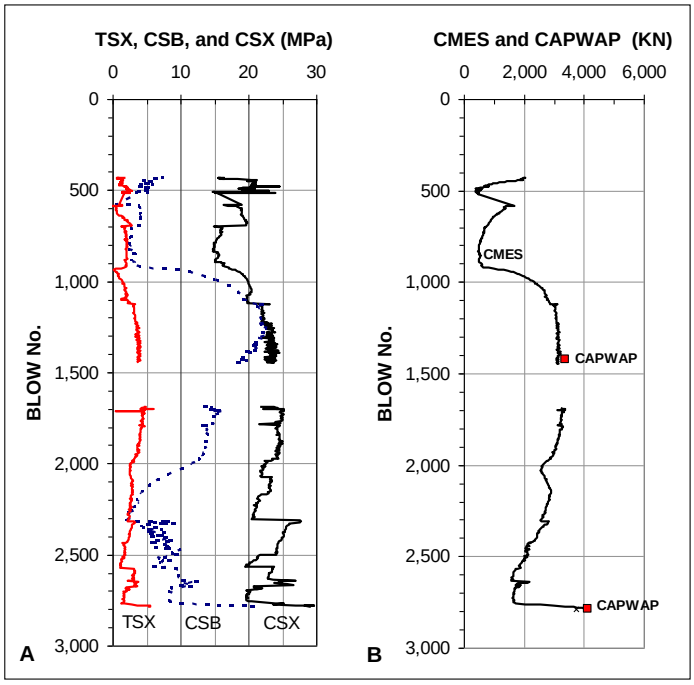

Fig. B PDA diagrams. **A**. Tension (TSX), toe stress (CSB) and maximum stress (CSX). **B**. CMES (RX4) and CAPWAP determined capacities.

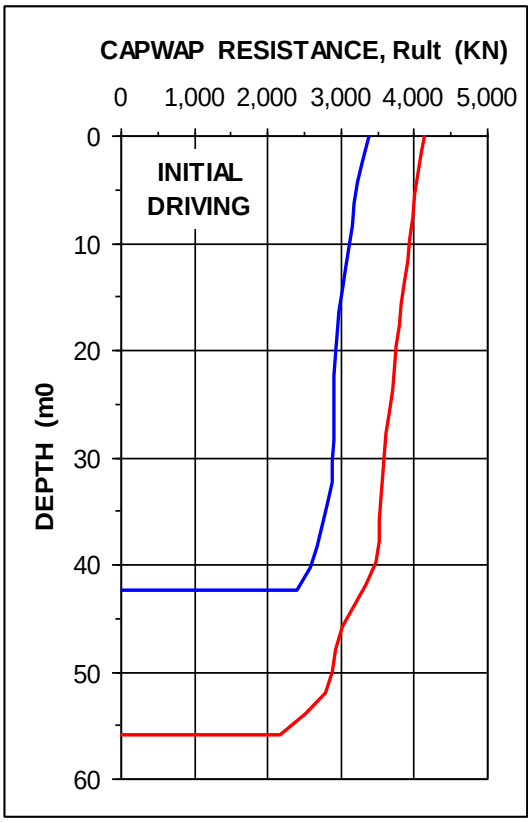

Fig. C CAPWAP determined resistance distribution at initial driving of the Shinho pile at depth 42 m and at end-of-driving at depth 56 m.